CLNS 03/1813
CLEO 03-01

Measurements of the branching fractions and helicity amplitudes in $B \to D^*\rho$ decays

S. E. Csorna,[1] I. Danko,[1] G. Bonvicini,[2] D. Cinabro,[2] M. Dubrovin,[2] S. McGee,[2] A. Bornheim,[3] E. Lipeles,[3] S. P. Pappas,[3] A. Shapiro,[3] W. M. Sun,[3] A. J. Weinstein,[3] R. A. Briere,[4] G. P. Chen,[4] T. Ferguson,[4] G. Tatishvili,[4] H. Vogel,[4] N. E. Adam,[5] J. P. Alexander,[5] K. Berkelman,[5] V. Boisvert,[5] D. G. Cassel,[5] P. S. Drell,[5] J. E. Duboscq,[5] K. M. Ecklund,[5] R. Ehrlich,[5] R. S. Galik,[5] L. Gibbons,[5] B. Gittelman,[5] S. W. Gray,[5] D. L. Hartill,[5] B. K. Heltsley,[5] L. Hsu,[5] C. D. Jones,[5] J. Kandaswamy,[5] D. L. Kreinick,[5] A. Magerkurth,[5] H. Mahlke-Krüger,[5] T. O. Meyer,[5] N. B. Mistry,[5] J. R. Patterson,[5] D. Peterson,[5] J. Pivarski,[5] S. J. Richichi,[5] D. Riley,[5] A. J. Sadoff,[5] H. Schwarthoff,[5] M. R. Shepherd,[5] J. G. Thayer,[5] D. Urner,[5] T. Wilksen,[5] A. Warburton,[5] M. Weinberger,[5] S. B. Athar,[6] P. Avery,[6] L. Breva-Newell,[6] V. Potlia,[6] H. Stoeck,[6] J. Yelton,[6] K. Benslama,[7] B. I. Eisenstein,[7] G. D. Gollin,[7] I. Karliner,[7] N. Lowrey,[7] C. Plager,[7] C. Sedlack,[7] M. Selen,[7] J. J. Thaler,[7] J. Williams,[7] K. W. Edwards,[8] D. Besson,[9] X. Zhao,[9] S. Anderson,[10] V. V. Frolov,[10] D. T. Gong,[10] Y. Kubota,[10] S. Z. Li,[10] R. Poling,[10] A. Smith,[10] C. J. Stepaniak,[10] J. Urheim,[10] Z. Metreveli,[11] K.K. Seth,[11] A. Tomaradze,[11] P. Zweber,[11] S. Ahmed,[12] M. S. Alam,[12] J. Ernst,[12] L. Jian,[12] M. Saleem,[12] F. Wappler,[12] K. Arms,[13] E. Eckhart,[13] K. K. Gan,[13] C. Gwon,[13] K. Honscheid,[13] D. Hufnagel,[13] H. Kagan,[13] R. Kass,[13] T. K. Pedlar,[13] E. von Toerne,[13] M. M. Zoeller,[13] H. Severini,[14] P. Skubic,[14] S.A. Dytman,[15] J.A. Mueller,[15] S. Nam,[15] V. Savinov,[15] J. W. Hinson,[16] J. Lee,[16] D. H. Miller,[16] V. Pavlunin,[16] B. Sanghi,[16] E. I. Shibata,[16] I. P. J. Shipsey,[16] D. Cronin-Hennessy,[17] A.L. Lyon,[17] C. S. Park,[17] W. Park,[17] J. B. Thayer,[17] E. H. Thorndike,[17] T. E. Coan,[18] Y. S. Gao,[18] F. Liu,[18] Y. Maravin,[18] R. Stroynowski,[18] M. Artuso,[19] C. Boulahouache,[19] S. Blusk,[19] K. Bukin,[19] E. Dambasuren,[19] R. Mountain,[19] H. Muramatsu,[19] R. Nandakumar,[19] T. Skwarnicki,[19] S. Stone,[19] J.C. Wang,[19] and A. H. Mahmood[20]

(CLEO Collaboration)

[1]*Vanderbilt University, Nashville, Tennessee 37235*
[2]*Wayne State University, Detroit, Michigan 48202*
[3]*California Institute of Technology, Pasadena, California 91125*
[4]*Carnegie Mellon University, Pittsburgh, Pennsylvania 15213*
[5]*Cornell University, Ithaca, New York 14853*
[6]*University of Florida, Gainesville, Florida 32611*
[7]*University of Illinois, Urbana-Champaign, Illinois 61801*
[8]*Carleton University, Ottawa, Ontario, Canada K1S 5B6 and the Institute of Particle Physics, Canada M5S 1A7*
[9]*University of Kansas, Lawrence, Kansas 66045*
[10]*University of Minnesota, Minneapolis, Minnesota 55455*
[11]*Northwestern University, Evanston, Illinois 60208*
[12]*State University of New York at Albany, Albany, New York 12222*
[13]*Ohio State University, Columbus, Ohio 43210*
[14]*University of Oklahoma, Norman, Oklahoma 73019*
[15]*University of Pittsburgh, Pittsburgh, Pennsylvania 15260*

[16]Purdue University, West Lafayette, Indiana 47907
[17]University of Rochester, Rochester, New York 14627
[18]Southern Methodist University, Dallas, Texas 75275
[19]Syracuse University, Syracuse, New York 13244
[20]University of Texas - Pan American, Edinburg, Texas 78539

(Dated: January 15, 2003)

Abstract

Using 9.1 fb^{-1} of e^+e^- data collected at the $\Upsilon(4S)$ with the CLEO detector using the Cornell Electron Storage Ring, measurements are reported for both the branching fractions and the helicity amplitudes for the decays $B^- \to D^{*0}\rho^-$ and $\bar{B}^0 \to D^{*+}\rho^-$. The fraction of longitudinal polarization in $\bar{B}^0 \to D^{*+}\rho^-$ is found to be consistent with that in $\bar{B}^0 \to D^{*+}\ell^-\bar{\nu}$ at $q^2 = M_\rho^2$, indicating that the factorization approximation works well. The longitudinal polarization in the B^- mode is similar. The measurements also show evidence of non-trivial final-state interaction phases for the helicity amplitudes.

Hadronic decays of heavy mesons are complicated by final-state interactions (FSI) which result from strong re-scattering of the products of the weak decay process. FSI effects may be less important if the final state is easy to produce directly via weak decay. It is also argued that if the final-state hadrons separate rapidly, due to a large energy release, there is little time for interaction. The factorization hypothesis, widely used in heavy-quark physics for hadronic two-body decays [1], assumes that the two hadronic currents may be treated independently of each other, neglecting FSI. In particular, the BSW model [1] utilizes this approximation in assuming that the short and long distance QCD contributions can be factorized. However, the validity of the factorization hypothesis has not been demonstrated by any rigorous theoretical calculation.

Körner and Goldstein [2] suggest a test of the factorization hypothesis by examining the polarization in B meson decays into two vector mesons. The idea is that, under the factorization hypothesis, certain hadronic decays are analogous to similar semileptonic decays evaluated at a fixed value of the momentum transfer, $q^2 \equiv M^2_{\ell\bar{\nu}}$. For instance, the polarization of the D^{*+} meson in $\bar{B}^0 \to D^{*+}\rho^-$ should equal that in $\bar{B}^0 \to D^{*+}l^-\bar{\nu}$ at $q^2 = M^2_\rho$. Specifically:

$$\frac{\Gamma_L}{\Gamma}(\bar{B}^0 \to D^{*+}\rho^-) = \frac{\Gamma_L}{\Gamma}(\bar{B}^0 \to D^{*+}\ell^-\bar{\nu})\Big|_{q^2=M^2_\rho}. \tag{1}$$

Here, Γ_L/Γ is the fraction of longitudinal polarization.

The differential decay rate for $B \to D^*\rho^-$ can be expressed in terms of three complex helicity amplitudes H_0, H_+ and H_- as:

$$\begin{aligned}\frac{d^3\Gamma}{d\cos\theta_{D^*}\,d\cos\theta_\rho d\chi} = \frac{9}{32\pi} \times \Big\{&4|H_0|^2\cos^2\theta_{D^*}\cos^2\theta_\rho + \left(|H_+|^2+|H_-|^2\right)\sin^2\theta_{D^*}\sin^2\theta_\rho \\ &+2\left[\Re(H_+H_-^*)\cos 2\chi - \Im(H_+H_-^*)\sin 2\chi\right]\sin^2\theta_{D^*}\sin^2\theta_\rho \\ &+\left[\Re(H_+H_0^*+H_-H_0^*)\cos\chi - \Im(H_+H_0^*-H_-H_0^*)\sin\chi\right]\sin 2\theta_{D^*}\sin 2\theta_\rho\Big\},\end{aligned} \tag{2}$$

where: θ_{D^*} is the decay angle of the D^0 in the D^* rest frame with respect to the D^* line of flight in the B rest frame; θ_ρ is the decay angle of the π^- in the ρ^- rest frame with respect to the ρ^- line of flight in the B rest frame; χ is the angle between the decay planes of the D^* and ρ; and $\Re(x)$ and $\Im(x)$ denote the real and imaginary parts of x, respectively.

The longitudinal and transverse polarizations are then defined as:

$$\frac{\Gamma_L}{\Gamma} = \frac{|H_0|^2}{|H_0|^2+|H_+|^2+|H_-|^2}, \tag{3}$$

and

$$\frac{\Gamma_T}{\Gamma} = 1 - \frac{\Gamma_L}{\Gamma}, \tag{4}$$

respectively.

Previous measurements have been performed on the $D^*\rho$ system. Using 0.89 fb^{-1} of $\Upsilon(4S)$ data and performing an unbinned two-dimensional likelihood fit to the joint $(\cos\theta_{D^*}, \cos\theta_\rho)$ distribution, the CLEO Collaboration measured $\Gamma_L/\Gamma = 0.93 \pm 0.05 \pm 0.05$ [3]. Later, using 3.1 fb^{-1} of $\Upsilon(4S)$ data and performing an unbinned maximum likelihood fit to the joint three-dimensional $(\cos\theta_{D^*}, \cos\theta_\rho, \chi)$ distribution, along with the invariant B and ρ mass distributions, CLEO reported a preliminary result of $\Gamma_L/\Gamma = 0.878 \pm 0.034 \pm 0.030$ [4]. Both results are in agreement with the theoretical prediction of 0.895 ± 0.019 for $\bar{B}^0 \to D^{*+}\rho^-$ [5].

Testing the factorization hypothesis would benefit from further reduction of the experimental uncertainty. We report here an improved measurement using ten times the data of the first measurement. This represents the final update of the second analysis and uses largely the same technique, but with some important improvements in both the event selection and the treatment of acceptance. Our results include the data used in the previous analyses and hence supersede them.

The data used in this analysis were collected at the Cornell Electron Storage Ring (CESR) with the CLEO detector in two configurations, known as CLEO II [6] and CLEO II.V [7]. The data consist of an integrated luminosity of 9.1 fb^{-1} collected at the $\Upsilon(4S)$ resonance, corresponding to 9.7×10^6 $B\bar{B}$ events, as well as 4.6 fb^{-1} of continuum data at energies just below the $\Upsilon(4S)$ resonance. The latter is used to study the backgrounds due to the non-resonant $e^+e^- \to q\bar{q}$ process.

In CLEO II, the momentum measurement of charged particles is carried out with a tracking system consisting of a six-layer straw-tube chamber, a ten-layer precision drift chamber, and a 51-layer main drift chamber. The tracking system operates inside a 1.5 T superconducting solenoid. For charged particles, the main drift chamber also provides a measurement of ionization energy loss (dE/dx), which is used for particle identification. The CLEO II.V detector was upgraded in two main aspects, both affecting charged particles. First, the straw-tube chamber was replaced with a three-layer double-sided silicon vertex detector; and second, the gas in the main drift chamber was changed from an argon-ethane to a helium-propane mixture. Photons are detected with a 7800-crystal CsI(Tl) electromagnetic calorimeter, which is also inside the solenoid. Muons are identified with proportional chambers placed at various depths within the steel return yoke of the magnet.

Charged tracks with momenta greater than 250 MeV/c are required to come from the interaction point and be well-measured (based on the quality of the track fit and the number of hits). Identified electrons and muons are excluded, and pions and kaons are required to have a measured dE/dx within 2.5 standard deviations (σ) of their expected values. To keep the efficiency high, softer tracks are only required to satisfy a looser requirement of consistency with originating at the interaction point. The π^0 candidates are formed from pairs of photons with an invariant mass within 2.5 standard deviations of the known π^0 mass. These pairs are then kinematically fitted with their invariant mass constrained to the known π^0 mass. The χ^2 of this kinematic fit must be less than nine. To suppress background from fake photons, the constituent photons of the π^0 must be detected in the central barrel calorimeter (which has the least material shadowing it) and have a minimum energy of $30 - 65$ MeV, depending on the source (D^{*0}, D^0, or ρ^-) of the π^0.

We reconstruct candidate D^{*0} and D^{*+} mesons in the modes $D^{*0} \to D^0\pi^0$ and $D^{*+} \to D^0\pi^+$, with $D^0 \to K^-\pi^+$, $D^0 \to K^-\pi^+\pi^0$, or $D^0 \to K^-\pi^+\pi^-\pi^+$. Throughout this paper, charge conjugate modes are implied. The reconstructed $D^* - D$ mass differences and the D^0 invariant mass are required to be within 2.5σ of the nominal values. The resolutions of these quantities are obtained from Monte Carlo simulations, and the $D^0 \to K^-\pi^+\pi^0$ resolution includes a π^0 energy dependence. We also require the $D^0 \to K^-\pi^+\pi^0$ candidates to come from the more densely populated regions of the Dalitz plot to suppress combinatoric background. Candidate ρ^- mesons are selected from $\pi^-\pi^0$ combinations which have an invariant mass within 150 MeV/c^2 of the nominal ρ^- mass.

The B^- and $\bar{B}^0$ mesons are reconstructed by combining the D^{*0} or D^{*+} candidates with the ρ^-. We calculate a beam-constrained B mass by substituting the beam energy (E_b) for the measured B^- or $\bar{B}^0$ candidate energy ($\sum_i E_i$): $M \equiv \sqrt{E_b^2 - {p_B}^2}$, where p_B is the measured momentum of the B candidate. This improves the M resolution by one order of magnitude, to about 3 MeV$/c^2$. The difference between the reconstructed energy of the B^- or $\bar{B}^0$ candidates and the beam energy, $\Delta E = \sum_i E_i - E_b$, is required to be 0 to within 2.5σ. The resolution of the energy difference varies from 10 MeV to 35 MeV, depending on the decay mode, and is also obtained from Monte Carlo simulations. We also account for the dependence of our ΔE resolution on the π^0 (from the ρ^- decay) energy, parameterizing it as a function of $\cos\theta_\rho$.

To suppress background from the continuum under the $\Upsilon(4S)$ resonance, only events with a ratio of Fox-Wolfram moments [8], $R_2 < 0.5$, are used, taking advantage of the fact that this ratio is larger for the more jet-like events from the continuum than the more spherical events from $B\bar{B}$ decays of the $\Upsilon(4S)$. We require that the polar angle of the reconstructed B satisfies $|\cos\theta_B| < 0.95$, given the known $\sin^2\theta_B$ distribution for $\Upsilon(4S)$ decay. Finally, a requirement is made on the cosine of the sphericity angle, Θ_S, defined as the angle between the sphericity axis of the B decay products and the rest of the particles in the event. Because of their two-jet structure, continuum events peak strongly at $|\cos\Theta_S| = 1$, while signal events are flat. Only candidates with $|\cos\Theta_S|$ below a maximum allowed value, dependent on the D^0 decay mode, are retained.

To measure both the branching fractions and the polarization in the decay of $B \to D^*\rho$, we perform an unbinned maximum likelihood fit to extract the number of signal events and the helicity amplitudes from the data. Events from the three D^0 decay modes are combined in the fit. The likelihood function, $\mathcal{L}$, has the form:

$$\mathcal{L} = \prod_{j=1}^{3} \frac{e^{-\nu_j}\nu_j^{n_j}}{n_j!} \prod_{i=1}^{n_j} \frac{n_j^S \cdot \mathcal{P}_{ji}^S(M, m, \cos\theta_{D^*}, \cos\theta_\rho, \chi) + n_j^B \cdot \mathcal{P}_{ji}^B(M, m, \cos\theta_{D^*}, \cos\theta_\rho, \chi)}{n_j^S + n_j^B}, \tag{5}$$

where m is the invariant mass of the candidate ρ^- meson, n_j^S and n_j^B are the number of signal and background events for the j-th D^0 decay mode, respectively ($\nu_j = n_j^S + n_j^B$), and n_j is the total number of data events for the j-th D^0 decay mode.

The signal probability distribution function, $\mathcal{P}_{ji}^S(M, m, \cos\theta_{D^*}, \cos\theta_\rho, \chi)$, is composed of two parts. The mass distribution part is a product of the beam-constrained B invariant mass distribution (assumed to have a Gaussian probability distribution) and a Blatt-Weisskopf form-factor-modeled [9] Breit-Wigner shape for the ρ^- invariant mass distribution; the angular distribution part is given by Eq. (2), multiplied by the detector acceptance, $\epsilon(\cos\theta_{D^*}, \cos\theta_\rho, \chi)$.

The background probability distribution function, $\mathcal{P}_{ji}^B(M, m, \cos\theta_{D^*}, \cos\theta_\rho, \chi)$, also has two components: the product of an ARGUS-type background function [10] for the beam-constrained B invariant mass and a flat distribution for the $\pi^-\pi^0$ invariant mass distribution; and an angular distribution for the background determined from events in the B mass sideband, defined as $5.200 < M < 5.265$ GeV$/c^2$. The background shape is parameterized as a product of second-order polynomials in $\cos\theta_{D^*}$ and $\cos\theta_\rho$ and the function $1+P_\chi\cos(\chi+\chi_0)$ in χ, where P_χ and χ_0 are allowed to vary in the fit to the sideband data.

To extract the number of signal and background events, the reconstructed candidates with $5.20 < M < 5.30$ GeV$/c^2$ are fit, and the angular distributions in both the signal and background probability density functions are ignored. Figure 1 shows the beam-constrained mass distributions for both B^- and $\bar{B}^0$.

The efficiencies of the B selection procedure for the three D^0 decay modes are determined from Monte Carlo simulations. Table I gives the number of signal events and the efficiencies,

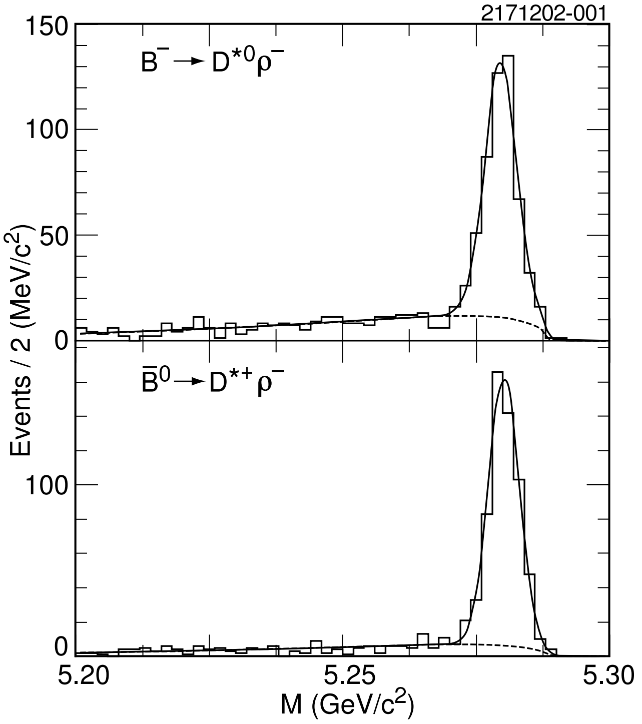

FIG. 1: B^- (top) and $\bar{B}^0$ (bottom) candidate mass distributions from the data, along with the results of the fits. Dashed curves indicate the ARGUS-type background.

where the uncertainties are statistical only.

TABLE I: Number of signal events and the efficiencies for $B^- \to D^{*0}\rho^-$ and $\bar{B}^0 \to D^{*+}\rho^-$ for the three D^0 decay modes. The uncertainties shown are statistical only.

B type	D^0 decay mode	n^S	ϵ (%)
B^-	$K^-\pi^+$	148.9 ± 13.8	6.56 ± 0.04
	$K^-\pi^+\pi^0$	177.4 ± 16.6	2.20 ± 0.02
	$K^-\pi^+\pi^-\pi^+$	136.0 ± 15.2	3.04 ± 0.03
$\bar{B}^0$	$K^-\pi^+$	196.3 ± 14.6	10.88 ± 0.05
	$K^-\pi^+\pi^0$	196.1 ± 16.4	3.67 ± 0.03
	$K^-\pi^+\pi^-\pi^+$	170.6 ± 13.9	4.46 ± 0.03

Assuming equal production of B^+B^- and $B^0\bar{B}^0$ at the $\Upsilon(4S)$, the resulting measured branching fractions are $\mathcal{B}(B^- \to D^{*0}\rho^-) = (0.98 \pm 0.06 \pm 0.16 \pm 0.05)\%$ and $\mathcal{B}(\bar{B}^0 \to D^{*+}\rho^-) = (0.68 \pm 0.03 \pm 0.09 \pm 0.02)\%$, which compare well with previous measurements [3], the recent BaBar measurement [11], and the world average [12]. A statistical uncertainty and two systematic uncertainties are quoted in the branching fractions. The first systematic error includes uncertainties in the number of produced $B\bar{B}$ pairs (2%), the background shape (3%), our Monte Carlo statistics ($1-2\%$), and the charged particle tracking and π^0 detection efficiencies ($10-18\%$). The second systematic error comes from uncertainties in the D^* and D^0 decay branching fractions. The contributions from non-resonant $D^*\pi\pi^0$ and other non-ρ^- components are small [3] and neglected. The contribution from the helicity amplitude dependence of the efficiency is less than 11% of the corresponding contribution from the Monte Carlo statistics, and hence, is also ignored.

These branching fraction measurements and the BSW prediction for $\mathcal{B}(B^- \to D^{*0}\rho^-)/\mathcal{B}(\bar{B}^0 \to D^{*+}\rho^-)$ [13], can be used to extract the ratio of the effective coupling strengths for color-suppressed modes (a_2) and color-enhanced modes (a_1) for the $D^*\rho$ final state. The extraction of a_2/a_1 is sensitive to the B^+B^- and $B^0\bar{B}^0$ production fractions; we used $f_{+-}/f_{00} = 1.072 \pm 0.045 \pm 0.027 \pm 0.024$ [12]. Our data give $a_2/a_1 = 0.21 \pm 0.03 \pm 0.05 \pm 0.04 \pm 0.04$, where the fourth uncertainty, from f_{+-}/f_{00}, is important here since other experimental systematics partially cancel. This result is in good agreement with the previous CLEO measurement [3] and others [14].

To extract the helicity amplitudes from the data, only the reconstructed B events in the B signal region (defined as $5.27 < M < 5.30$ GeV/c^2) are included in the fit. The number of signal and background events for the three D^0 decay modes are taken from the previous mass fit, with the latter scaled to the B signal region.

The dependence of the acceptance on the decay angles, combined with the effects of detector resolution, are determined from Monte Carlo simulations. Due to the *a priori* unknown helicity amplitudes, a weighting technique based on Eq. (2) is employed to adjust the acceptance for different helicity amplitudes. Fits are iterated until the helicity amplitudes used for weighting and those resulting from the fit converge. Our study shows that the acceptance over the angle χ is quite flat and thus the acceptance can be factorized as $\epsilon(\cos\theta_{D^*}, \cos\theta_\rho, \chi) = \epsilon_2(\cos\theta_{D^*}, \cos\theta_\rho)\epsilon_1(\chi)$ with $\epsilon_1(\chi) = Q_0(1 + Q_1 \sin\chi + Q_2 \cos\chi + Q_3 \sin 2\chi + Q_4 \cos 2\chi)$ and $Q_{1,2,3,4}$ are all found to be small. We use the following functional form to fit the two-dimensional acceptance from the weighted Monte Carlo:

$$\begin{aligned}
&\epsilon_2(\cos\theta_{D^*}, \cos\theta_\rho) = \\
&\qquad \epsilon_{00} \frac{1 + P_1 \cos^2\theta_{D^*} + P_2 \cos^2\theta_\rho + P_3 \cos^2\theta_{D^*} \cos^2\theta_\rho}{1 + P_{10} \cos^2\theta_{D^*} + P_{11} \cos^2\theta_\rho + P_{12} \cos^2\theta_{D^*} \cos^2\theta_\rho} \\
&\qquad \cdot \exp(-P_4 \cos\theta_{D^*} - P_5 \cos^2\theta_{D^*} - P_6 \cos^3\theta_{D^*} - P_7 \cos\theta_\rho - P_8 \cos^2\theta_\rho - P_9 \cos^3\theta_\rho).
\end{aligned} \tag{6}$$

This gives an excellent fit with no discernible pattern of residuals.

Performing the unbinned maximum likelihood fit, we obtain the helicity amplitudes for the decay $B \to D^*\rho$ listed in Table II. Figure 2 shows the one-dimensional angular distributions and the projections from the fit. The errors quoted in the table are the statistical and systematic uncertainties, respectively.

The sources of systematic uncertainty are the acceptance parameterization, detector smearing, background level and shape, non-resonant $\pi^-\pi^0$ contribution, and the polarization dependence on the mass of the ρ^- meson. Their individual contributions are shown in Table III. For the acceptance parameterization, we use different functional forms for both $\epsilon_2(\cos\theta_{D^*}, \cos\theta_\rho)$ and $\epsilon_1(\chi)$ in the maximum likelihood fit, and the changes of the helicity amplitudes are taken as the systematic uncertainties. To gauge the effect of detector smearing, we increase the smearing in the nominal Monte Carlo by a conservative 15% of itself. We increase the number of background events for each D^0 decay mode independently by 1σ and use the observed shifts as the corresponding systematic uncertainties. Our largest systematic uncertainty comes from the shape of the background angular distribution. We compare the nominal fit results to three other fits: one with the background flat in the decay angles, one with the shape fit to the Monte Carlo events in the M sideband, and one with the shape fit to the non-signal Monte Carlo events in the M peak region. The largest variation

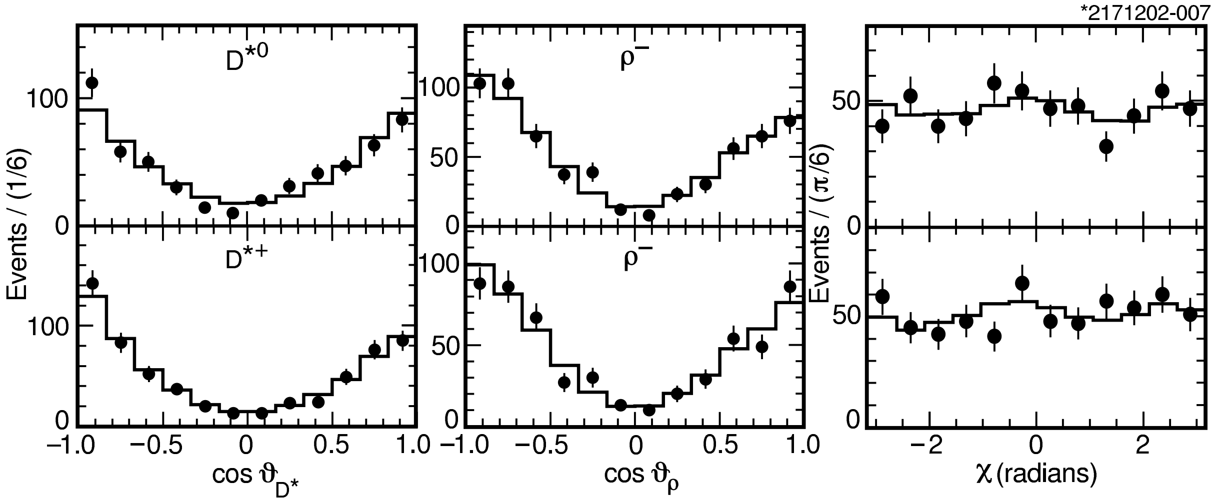

FIG. 2: The $\cos\theta_{D^*}$ (left), $\cos\theta_\rho$ (middle) and χ (right) distributions for $B^- \to D^{*0}\rho^-$ (top) and $\bar{B}^0 \to D^{*+}\rho^-$ (bottom) from the data (dots) and the corresponding fit projections (histograms).

TABLE II: The measured helicity amplitudes for $B^- \to D^{*0}\rho^-$ and $\bar{B}^0 \to D^{*+}\rho^-$. The phase of H_0 is fixed to zero in each mode. α_+ and α_- are the phases, in radians, of H_+ and H_-, respectively: $H_\pm = |H_\pm| \exp(i\alpha_\pm)$.

Quantity	$B^- \to D^{*0}\rho^-$	$\bar{B}^0 \to D^{*+}\rho^-$
$\|H_0\|$	$0.944 \pm 0.009 \pm 0.009$	$0.941 \pm 0.009 \pm 0.006$
$\|H_+\|$	$0.122 \pm 0.040 \pm 0.010$	$0.107 \pm 0.031 \pm 0.011$
α_+	$1.02 \pm 0.28 \pm 0.11$	$1.42 \pm 0.27 \pm 0.04$
$\|H_-\|$	$0.306 \pm 0.030 \pm 0.025$	$0.322 \pm 0.025 \pm 0.016$
α_-	$0.65 \pm 0.16 \pm 0.04$	$0.31 \pm 0.12 \pm 0.04$

among these three is taken as the systematic uncertainty. To account for a background contribution from non-resonant $\pi^-\pi^0$ combinations in the data sample, an $S-$wave component with a flat angular distribution is added in the helicity angular distribution. Finally, we include a systematic uncertainty due to our sensitivity to the q^2 dependence of the helicity amplitudes. In the nominal fit, we ignore this possible dependence. Instead, we relate the helicity amplitudes at a momentum transfer $q^2 = M_\rho^2$ to the actual q^2 of the events, using the factorization hypothesis, and we use the shifts as the uncertainty. The total systematic uncertainty is then the sum of the above contributions in quadrature.

As can be seen from Table II, our results indicate possible non-trivial helicity amplitude phases, α_+ and α_-. To better gauge the significance of such a conclusion, we use the quantity $\sqrt{\Delta(-2\ln\mathcal{L}_{max})}$, where Δ refers to the increase in $-2\ln\mathcal{L}_{max}$ when both phases are forced to be zero, as compared to the nominal fit with floating phases. Interpreting this quantity as the net statistical significance of non-zero phases, we find 3.19σ and 2.75σ for $B^- \to D^{*0}\rho^-$ and $\bar{B}^0 \to D^{*+}\rho^-$, respectively. The stability of the significance is evaluated by examining the changes in $\sqrt{\Delta(-2\ln\mathcal{L}_{max})}$ for all of the systematic variations discussed above. The values are quite stable, ranging from $3.09 - 3.54\sigma$ and $2.65 - 2.83\sigma$ for B^-

TABLE III: Summary of the systematic uncertainties for the helicity amplitudes of $B^- \to D^{*0}\rho^-$ and $\bar{B}^0 \to D^{*+}\rho^-$, respectively.

$D^{*0}\rho^-$	All $\times 10^{-2}$						
Quantity	Accep.	Smearing	Bkg. level	Bkg. shape	Non-res.	q^2 dep.	Total
$\|H_0\|$	0.08	0.06	0.13	0.83	0.01	0.07	0.85
$\|H_+\|$	0.32	0.25	0.37	0.60	0.23	0.43	0.95
α_+	2.23	1.90	2.96	9.82	0.71	1.59	10.81
$\|H_-\|$	0.24	0.28	0.30	2.45	0.08	0.03	2.50
α_-	1.29	1.12	2.22	1.07	1.02	2.84	4.25
Γ_L/Γ	0.14	0.11	0.25	1.58	0.01	0.12	1.62
$D^{*+}\rho^-$	All $\times 10^{-2}$						
Quantity	Accep.	Smearing	Bkg. level	Bkg. shape	Non-res.	q^2 dep.	Total
$\|H_0\|$	0.07	0.01	0.04	0.61	0.13	0.10	0.63
$\|H_+\|$	0.25	0.01	0.09	0.92	0.44	0.09	1.06
α_+	2.17	0.18	1.64	2.12	2.17	1.35	4.29
$\|H_-\|$	0.20	0.03	0.13	1.52	0.06	0.26	1.56
α_-	0.92	0.01	0.39	3.95	0.18	0.16	4.08
Γ_L/Γ	0.13	0.02	0.07	1.14	0.25	0.19	1.19

and $\bar{B}^0$, respectively. Previously, indications of FSI phases have also been reported in the $D\pi$ [15] and the $J/\psi K^*$ systems [16].

The results for the helicity amplitudes correspond to

$$\begin{cases} \dfrac{\Gamma_L}{\Gamma}(B^- \to D^{*0}\rho^-) &= 0.892 \pm 0.018 \pm 0.016, \\ \dfrac{\Gamma_L}{\Gamma}(\bar{B}^0 \to D^{*+}\rho^-) &= 0.885 \pm 0.016 \pm 0.012, \end{cases} \tag{7}$$

where the two uncertainties are statistical and systematic, respectively. Within the uncertainties, the fraction of longitudinal polarization for $\bar{B}^0 \to D^{*+}\rho^-$ is in good agreement with the previous CLEO measurement [3] and with the HQET prediction of 0.895 ± 0.019 [5] using factorization and the measurements of the semileptonic form factors. Longitudinal polarization as a function of q^2 is plotted in Figure 3 for such a prediction and compared with our new $D^{*+}\rho^-$ result, as well as previous measurements for $D^{*+}\rho'^-$ [17] and $D^{*+}D_s^{*-}$ [18]. The agreement is excellent, indicating that the factorization hypothesis works well at the level of the current uncertainties.

In summary, we have measured both the branching fractions and the helicity amplitudes for $B \to D^*\rho$. The values of the branching fractions, the ratio a_2/a_1, and the degree of longitudinal polarization are in good agreement with previous measurements and with theoretical predictions. The measurement of the fraction of longitudinal polarization confirms the validity of the factorization assumption at relatively low q^2. Finally, the measurement of the helicity amplitudes indicates a strong possibility of non-trivial helicity amplitude phases which would arise from final-state interactions. Such phases are of interest since they are required for the observation of direct CP violation in B decay rates [20].

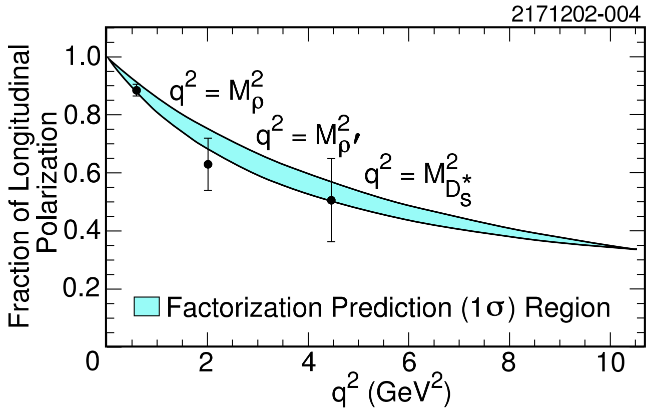

FIG. 3: The fraction of longitudinal polarization in $\bar{B}^0 \to D^{*+}X$ decays as a function of $q^2 = M_X^2$, where X is a vector meson. Shown are the current $\bar{B}^0 \to D^{*+}\rho^-$ polarization measurement, and earlier measurements of $\bar{B}^0 \to D^{*+}\rho'^-$ [17], and $\bar{B}^0 \to D^{*+}D_s^{*-}$ [18]. The shaded region represents the prediction using factorization and HQET, and extrapolating from the semileptonic $\bar{B}^0 \to D^{*+}\ell^-\bar{\nu}$ form factor results [19]. The shaded contour shows a one standard deviation variation in the theoretical prediction.

We gratefully acknowledge the effort of the CESR staff in providing us with excellent luminosity and running conditions. We thank Lalith Perera for contributions to a preliminary version of this analysis. M. Selen thanks the Research Corporation, and A.H. Mahmood thanks the Texas Advanced Research Program. This work was supported by the National Science Foundation, and the U.S. Department of Energy.

---

[1] M. Bauer, B. Stech and M. Wirbel, Z. Phys. C **34**, 103 (1987).

[2] J. Körner and G. Goldstein, Phys. Lett. **89 B**, 105 (1979).

[3] CLEO Collaboration, M.S. Alam *et al.*, Phys. Rev. **D 50**, 43 (1994).

[4] CLEO Collaboration, G. Bonvicini *et al.*, CLEO CONF 98-23, International Conference on High-Energy Physics (Vancouver, 1998).

[5] J.L. Rosner, Phys. Rev. **D 42**, 3732 (1990); M. Neubert, Phys. Lett. **B 264**, 455 (1991); G. Kramer, T. Mannel and W.F. Palmer, Z. Phys. **C 55**, 497 (1992); J.D. Richman, in *Probing the Standard Model of Particle Interactions*, edited by R. Gupta, A. Morel, E. de Rafael, and F. David (Elsevier, Amsterdam, 1999), p. 640.

[6] CLEO Collaboration, Y. Kubota *et al.*, Nucl. Instrum. Methods Phys. Res., Sect. **A 320**, 66 (1992).

[7] T.S. Hill, Nucl. Instrum. Methods Phys. Res., Sect. **A 418**, 32 (1998).

[8] G. Fox and S. Wolfram, Phys. Rev. Lett. **41**, 1581 (1978).

[9] V.F. Weisskopf and J.M. Blatt, *Theoretical Nuclear Physics*, p. 361 (Wiley, 1952).

[10] ARGUS Collaboration, H. Albrecht *et al.*, Phys. Lett. **B 241**, 278 (1990); **B 254**, 288 (1991).

[11] B. Brau, Int. J. Mod. Phys. **A 16**, Suppl. 1A 440 (2001).

[12] Particle Data Group, Phys. Rev. D **66**, 010001 (2002).

[13] M. Neubert, V. Rieckert, Q.P. Xu and B. Stech, in *Heavy Flavours*, edited by A.J. Buras and H. Lindner (World Scientific, Singapore, 1992).

[14] T.E. Browder and K. Honscheid, Prog. Part. Nucl. Phys. **35**, 81 (1995); Particle Data Group, Eur. Phys. J. **C 15**, 1 (2000).
[15] CLEO Collaboration, T.E. Coan *et al.*, Phys. Rev. Lett. **88**, 062001 (2002); CLEO Collaboration, S. Ahmed *et al.*, Phys. Rev. **D66**, 031101 (2002).
[16] CDF Collaboration, T. Affolder *et al.*, Phys. Rev. Lett. **85**, 4668 (2000).
[17] CLEO Collaboration, J.P. Alexander *et al.*, Phys. Rev. **D 64**, 092001 (2001).
[18] CLEO Collaboration, S. Ahmed *et al.*, Phys. Rev. **D 62**, 112003 (2000).
[19] CLEO Collaboration, J. Duboscq *et al.*, Phys. Rev. Lett. **76**, 3898 (1996).
[20] A.S. Dighe, I. Dunietz and R. Fleischer, Eur. Phys. J. **C 6**, 647 (1999).